AMERICAN ACADEMY OF OPHTHALMOLOGY
The Eye M.D. Association

Clinical and Molecular Characteristics of Childhood-Onset Stargardt Disease

Kaoru Fujinami, MD,[1,2,3,4] *Jana Zernant, MS,*[5] *Ravinder K. Chana, BSc,*[3,4] *Genevieve A. Wright, BSc,*[3,4] *Kazushige Tsunoda, MD, PhD,*[1] *Yoko Ozawa, MD, PhD,*[2] *Kazuo Tsubota, MD, PhD,*[2] *Anthony G. Robson, PhD,*[3,4] *Graham E. Holder, PhD,*[3,4] *Rando Allikmets, PhD,*[5,6] *Michel Michaelides, MD, FRCOphth,*[3,4,*] *Anthony T. Moore, FRCS, FRCOphth*[3,4,*]

Purpose: To describe the clinical and molecular characteristics of patients with childhood-onset Stargardt disease (STGD).

Design: Retrospective case series.

Participants: Forty-two patients who were diagnosed with STGD in childhood at a single institution between January 2001 and January 2012.

Methods: A detailed history and a comprehensive ophthalmic examination were undertaken, including color fundus photography, autofluorescence imaging, spectral-domain optical coherence tomography (SD-OCT), and pattern and full-field electroretinograms. The entire coding region and splice sites of *ABCA4* were screened using a next-generation, sequencing-based strategy. The molecular genetic findings of childhood-onset STGD patients were compared with those of adult-onset patients.

Main Outcome Measures: Clinical, imaging, electrophysiologic, and molecular genetic findings.

Results: The median ages of onset and the median age at baseline examination were 8.5 (range, 3–16) and 12.0 years (range, 7-16), respectively. The median baseline logarithm of the minimum angle of resolution visual acuity was 0.74. At baseline, 26 of 39 patients (67%) with available photographs had macular atrophy with macular/peripheral flecks; 11 (28%) had macular atrophy without flecks; 1 (2.5%) had numerous flecks without macular atrophy; and 1 (2.5%) had a normal fundus appearance. Flecks were not identified at baseline in 12 patients (31%). SD-OCT detected foveal outer retinal disruption in all 21 patients with available images. Electrophysiologic assessment demonstrated retinal dysfunction confined to the macula in 9 patients (36%), macular and generalized cone dysfunction in 1 subject (4%), and macular and generalized cone and rod dysfunction in 15 individuals (60%). At least 1 disease-causing *ABCA4* variant was identified in 38 patients (90%), including 13 novel variants; ≥2 variants were identified in 34 patients (81%). Patients with childhood-onset STGD more frequently harbored 2 deleterious variants (18% vs 5%) compared with patients with adult-onset STGD.

Conclusions: Childhood-onset STGD is associated with severe visual loss, early morphologic changes, and often generalized retinal dysfunction, despite often having less severe fundus abnormalities on examination. One third of children do not have flecks at presentation. The relatively high proportion of deleterious *ABCA4* variants supports the hypothesis that earlier onset disease is often owing to more severe variants in *ABCA4* than those found in adult-onset disease. *Ophthalmology 2015;122:326-334 © 2015 by the American Academy of Ophthalmology. This is an open access article under the CC BY license (http://creativecommons.org/licenses/by/3.0/).*

Supplemental material is available at www.aaojournal.org.

Stargardt macular dystrophy (STGD) is the most common form of juvenile-onset macular degeneration; it is inherited as an autosomal-recessive trait and caused by mutations in the *ABCA4* gene.[1–3] Most cases present with central visual loss in early teenage years and ophthalmoscopy classically reveals macular atrophy with yellowish-white flecks at the posterior pole at the level of the retinal pigment epithelium (RPE).[1]

A large number of studies have described wide phenotypic variability and variable severity in *ABCA4*-associated retinopathy. The various phenotypes encompass macular atrophy without flecks, bull's-eye maculopathy, fundus flavimaculatus (retinal flecks without macular atrophy), a foveal sparing phenotype, cone-rod dystrophy, and "retinitis pigmentosa."[1–20] There is also considerable allelic heterogeneity, with >700 variants in *ABCA4* having been reported to date.[1,2,4–34]

Patients with childhood-onset STGD tend to develop early severe visual acuity (VA) loss, markedly compromised retinal function on electroretinography with generalized rod and cone system dysfunction, and rapid enlargement of RPE atrophy and progressive loss of retinal function.[5,10,13,35,36] Patients with adult-onset disease are more likely to retain useful VA for longer and show milder retinal dysfunction at diagnosis.[7,11,13,15,35] There have been no previous studies specifically describing the clinical findings in a large cohort

http://dx.doi.org/10.1016/j.ophtha.2014.08.012
ISSN 0161-6420/14

of molecularly confirmed STGD patients presenting and examined in childhood; the majority of previous reports relate to clinical features of patients examined in adulthood, some of whom may have had childhood-onset disease.

The purpose of this study was to describe the detailed clinical and molecular genetic findings of a large cohort of patients from a single center with childhood-onset STGD examined before 17 years of age.

Methods

Patients

Forty-two patients diagnosed with STGD at <17 years of age, between January 2001 and January 2012, were ascertained from the pediatric inherited retinal disease clinics at Moorfields Eye Hospital. Two subjects have been described in a previous case report.[9] Blood samples were collected and genomic DNA extracted from peripheral blood leukocytes after obtaining informed consent. The protocol of the study adhered to the provisions of the Declaration of Helsinki and was approved by the local Ethics Committee of Moorfields Eye Hospital.

Clinical Evaluation and Electrophysiology

A detailed medical history was obtained and a full ophthalmologic examination performed. The age of onset was defined as either the age at which visual loss was first noted by the patient or, in the "asymptomatic" patients, when an abnormal retinal appearance was first detected. The duration of disease was calculated as the difference between age at onset and age at most recent examination in childhood. The follow-up data were obtained before the age of 17 years.

Clinical evaluation included best-corrected VA, dilated ophthalmoscopy, color fundus photography, fundus autofluorescence imaging (AF), spectral-domain optical coherence tomography (SD-OCT), and electrophysiologic assessment. Best-corrected Snellen VA was converted to equivalent logarithm of the minimum angle of resolution (logMAR) VA. Follow-up data of logMAR VA, color fundus photography, and AF imaging were compared with those at baseline.

Color fundus photography was performed with a TRC-50IA Retinal Fundus Camera (Topcon, Tokyo, Japan). Patients were divided into 1 of 6 fundus appearance groups based on the presence and location of central (macular) RPE atrophy and yellowish-white flecks (Table 1).

Autofluorescence images before 2009 were obtained with an HRA 2 (Heidelberg Engineering, Heidelberg, Germany; excitation light, 488 nm, barrier filter, 500 nm; field of view, 30×30°); imaging after 2009 was undertaken using the Spectralis with viewing module version 5.1.2.0 (Heidelberg Engineering; excitation light, 488 nm; barrier filter, 500 nm; fields of view, 30×30° and 55×55°).[37] Patients were classified into 1 of 3 AF patterns, as previously described (Table 1).[6,36]

Spectral domain OCT was undertaken with the Spectralis with viewing module version 5.1.2.0. The HEYEX software interface (version 1.6.2.0; Heidelberg Engineering) was used for retinal thickness measurements.[6,37] Central foveal thickness was defined as the distance between the inner retinal surface and the inner border of the RPE.[6]

Electrophysiologic assessment included full-field electroretinogram (ERG), and pattern ERG, recorded with gold foil electrodes. Protocols incorporated the recommendations of the International Society for Clinical Electrophysiology of Vision.[38,39] Full-field ERGs were used to assess generalized rod and cone system function and included (i) dark-adapted dim flash 0.01 $cd \cdot s \cdot m^{-2}$ (DA 0.01), (ii) dark-adapted bright flash 11.0 $cd \cdot s \cdot m^{-2}$ (DA 11.0), (iii) light-adapted 3.0 $cd \cdot s \cdot m^{-2}$ 30 Hz flicker ERG (LA 3.0 30 Hz), and (iv) light-adapted 3.0 $cd \cdot s \cdot m^{-2}$ at 2 Hz (LA 3.0). The pattern ERG P50 component was used to assess macular function. All the components of the ERG and the pattern ERG P50

Table 1. Classification of Phenotype and Genotype in Stargardt Disease, Based on Fundus Appearance, Autofluorescence Pattern, Electrophysiologic Assessment, and *ABCA4* Variants

Fundus Appearance		AF Pattern		ERG Group		Genotype Group Classification	
Grade 1	Normal fundus	Type 1	Localized low AF signal at the fovea surrounded by a homogeneous background with/without perifoveal foci of high or low signal	Group 1	PERG abnormality with normal full-field ERGs	Genotype A	Two or more (likely) deleterious variants
Grade 2	Macular and/or peripheral flecks without central atrophy						
Grade 3a	Central atrophy without flecks	Type 2	Localized low AF signal at the macula surrounded by a heterogeneous background and widespread foci of high or low AF signal extending anterior to the vascular arcades	Group 2	PERG abnormality with additional generalized cone ERG abnormality	Genotype B	One deleterious variant and ≥1 missense or in-frame insertion/deletion variant(s)
Grade 3b	Central atrophy with macular and/or peripheral flecks						
Grade 3c	Paracentral atrophy with macular and/or peripheral flecks, without central atrophy						
Grade 4	Multiple extensive atrophic changes of the RPE, extending beyond the vascular arcades	Type 3	Multiple areas of low AF signal at posterior pole with a heterogeneous background and/or foci of high or low signal	Group 3	PERG abnormality with additional generalized cone and rod ERG abnormality	Genotype C	Two or more missense or in-frame insertion/deletion variants

AF = autofluorescence; ERG = electroretinography; PERG = pattern electroretinography; RPE = retinal pigment epithelium.
Aligned grades/types/groups of 4 classifications do not correlate with each other.

component were examined to classify patients into 1 of the 3 previously described electrophysiologic groups (Table 1).[5,35]

Mutation Screening

Blood samples were collected in EDTA tubes and DNA was extracted with a Nucleon Genomic DNA extraction kit (BACC2; Tepnel Life Sciences, West Lothian, UK).[8] All 50 exons and exon–intron boundaries of the *ABCA4* gene were amplified using Illumina Truseq Custom Amplicon protocol (Illumina, San Diego, CA), followed by sequencing on Illumina MiSeq platform.[8,22] The next-generation sequencing reads were analyzed and compared with the reference genome GRCh37/hg19, using the variant discovery software NextGENe (SoftGenetics LLC, State College, PA). All detected possibly disease-associated variants were confirmed by Sanger sequencing.[8,22]

All the missense variants identified were analyzed using 2 software prediction programs: SIFT (Sorting Intolerant from Tolerant; available from www.sift.jcvi.org/; accessed November 1, 2013), and PolyPhen2 (available from www.genetics.bwh.harvard.edu/pph/index.html; accessed November 1, 2013). Predicted effects on splicing of all the missense and intronic variants were assessed with the Human Splicing finder program version 2.4.1 (available from www.umd.be/HSF/; accessed November 1, 2013). The allele frequency of all variants was estimated by reference to the Exome Variant Server (NHLBI Exome Sequencing Project, Seattle, WA; available from www.snp.gs.washington.edu/EVS/; accessed November 1, 2013).

Patients harboring $\geq$2 mutations were classified into 3 genotype groups based on mutation type: Group A included patients with $\geq$2 definitely or likely deleterious (severe) variants; group B included patients with 1 deleterious variant and $\geq$1 missense or in-frame insertion/deletion variants; and group C included individuals with $\geq$2 missense or in-frame insertion/deletion variants[10] (Table 1). One disease-associated intronic change of unknown effect was treated as a deleterious allele owing to the associated severe clinical phenotype previously reported.[5,22] It should be noted, however, that assigning severity (e.g., a deleterious effect) to a mutation was not always straightforward, especially for missense alleles and some variants in splice sites.

Comparison Between Childhood-Onset and Adult-Onset STGD

To investigate differences between the patients with childhood-onset STGD and those with adult-onset STGD, clinical and molecular genetic data of patients with adult-onset STGD ascertained at Moorfields Eye Hospital were reviewed. The comparison group consisted of all patients who had adult-onset STGD (older than 17 years), and who had $\geq$2 disease-causing *ABCA4* variants.

Statistical analysis was performed using commercially available software: Excel Tokei 2010 (Social Survey Research Information Co., Ltd., Tokyo, Japan). The eye used for analysis was selected according to the Random Integer Generator (available from www.random.org/). The Mann–Whitney *U* test was applied to investigate the differences between the 2 groups (childhood-onset STGD vs adult-onset STGD) in terms of logMAR VA, and central foveal thickness. The chi square statistic was applied to investigate the association between selected categorical variables of childhood-onset and adult-onset disease, including fundus appearance, flecks (macular, peripheral, and no flecks), presence of pigmentation, AF pattern, electrophysiologic group, and genotype group. $P < 0.05$ was considered to indicate statistical significance.

Results

Forty-two unrelated patients with childhood-onset STGD were ascertained; the clinical findings are summarized in Table 2 (available at www.aaojournal.org). There were 22 female and 20 male patients. Eight (19%) were from consanguineous families. The median age of onset was 8.5 years (range, 3-16), and the median age at baseline examination was 12.0 years (range, 7–16). The median logMAR VA at baseline in all 42 patients was 0.74 in the right eye and 0.74 in the left eye (range, 0.10–1.30 and 0.12–1.40, respectively). The mean duration of disease at baseline was 2.0 years (range, 0–9). Follow-up data were available for logMAR VA, fundus photography, and AF imaging, in 24, 14, and 11 patients, respectively. The detailed changes in these parameters during follow-up are presented in Table 3 (available at www.aaojournal.org).

The median logMAR VA at baseline in the 24 patients that were monitored was 0.75 in the right eye and 0.75 in the left eye (range, 0.10–1.30 and 0.12–1.30, respectively); the median logMAR VA at follow-up was 1.00 in the right and 1.00 in the left eye (range, 0.05–1.40 and 0.20–1.60, respectively) at a median age of 15.0 years (range, 12–16). Fifteen patients (15/42; 36%) had logMAR or $\leq$1.0 VA in the better eye at baseline. Thirteen of 24 patients (54%) with available follow-up data had logMAR VA of $\leq$1.0 in the better eye at follow-up (range, 11–16). Follow-up data were available in 14 of 27 patients with VA better than logMAR 1.0 in the better eye at baseline; 6 (43%) had logMAR of $\leq$1.0 VA in the better eye at follow-up (range, 13–15).

Color fundus photographs, AF images, and SD-OCT images of 5 representative cases are shown in Figure 1. Baseline color fundus photographs were obtained in 39 patients (Table 2). Among the 39 patients, there was 1 (2.5%) with a grade 1 fundus appearance at baseline, 1 (2.5%) with grade 2, 11 (28%) with grade 3a, and 26 (67%) with grade 3b. There were no patients with a grade 3c or grade 4 fundus appearance. Central atrophy was present in 37 of the 39 patients (95%) at baseline; flecks were detected at the macula in 4 of the 39 patients (10%) and in the periphery in 23 (59%), with no visible flecks in 12 individuals (31%; Table 2). Retinal pigmentation was present in 2 of the 39 patients (5%; patients 24 and 34).

Serial color fundus photographs were available in 14 patients (Table 3), 3 of whom showed a fundus grade transition. Macular flecks, which were not present at baseline, developed in 2 subjects (patients 7 and 13) and macular and peripheral flecks became visible in 1 individual (patient 26). Color fundus photographs and AF images of 4 representative cases who developed flecks during the follow-up interval are shown in Figure 2.

Patients 17 and 18 had fine dots at the central macula surrounded by numerous peripheral flecks, classified into fundus grade 3b (patient 17; Fig 3). Clinical and molecular genetic data of these 2 patients have been previously described.[9] Only 1 patient had asymmetric fundus findings, with a central atrophic-appearing lesion with peripheral flecks extending anterior to the vascular arcades in the right eye, and macular atrophy with flecks, subretinal fibrosis, and hyperpigmentation at the level of RPE in the left eye (patient 29; Fig 3).

We obtained AF images for 32 patients at baseline (Table 2). There were 10 of the 32 patients (31%) with type 1 AF pattern, 22 (69%) with type 2 AF, and no subjects with type 3 AF. Serial AF images were obtained in 11 patients during the follow-up interval (Table 3); no patient demonstrated an AF grouping transition.

We obtained SD-OCT images for 21 patients at baseline (Table 2). Outer retinal disruption at the fovea was present in all 21 patients. The median central foveal thickness of the right and left eyes was 60.0 and 55.0 μm, respectively (range, 33–138 and

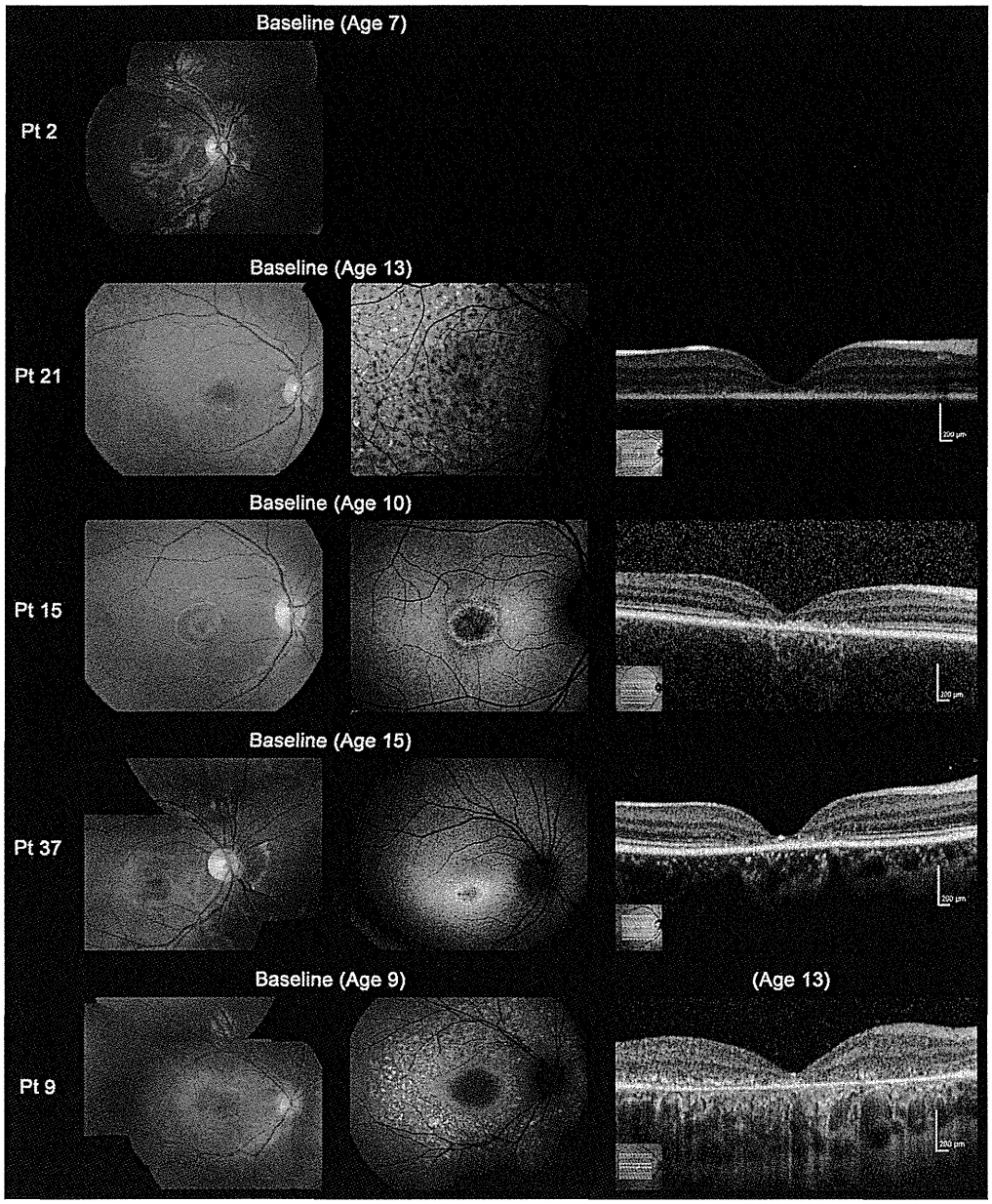

Figure 1. Color fundus photographs, autofluorescence, and spectral-domain optical coherence tomographic images of 5 representative cases with childhood-onset Stargardt Disease (patients 2, 21, 15, 37, and 9). Color fundus photographs of patient 2 shows normal findings at age 7 (fundus grade: 1). Patient 21 has numerous flecks at the posterior pole without central atrophy (fundus grade: 2) and autofluorescence (AF) imaging demonstrates widespread multiple foci of high and low AF signal at the posterior pole with a heterogeneous background (AF type 2). Spectral-domain optical coherence tomography (SD-OCT) identifies marked outer retinal loss at the central macula. Patient 15 has central atrophy without flecks (fundus grade: 3a) and AF imaging demonstrates a localized low AF signal at the fovea with a high signal edge surrounded by a homogeneous background (AF type: 1). SD-OCT detects marked outer retinal loss at the central macula. Patient 37 has central atrophy with macular flecks (fundus grade: 3b) and a localized low AF signal at the fovea surrounded by a homogeneous background with perifoveal foci of high signal (AF type: 1). SD-OCT shows outer retinal loss at the central macula. Patient 9 has central atrophy with peripheral flecks extending anterior to the vascular arcades (fundus grade: 3b) and a localized low AF signal at the macula surrounded by a heterogeneous background and widespread foci of high AF signal extending anterior to the vascular arcades (AF type: 2). SD-OCT reveals outer retinal disruption at the macula. Pt = patient.

35–140, respectively). Eighteen of the 21 patients (86%) had severe foveal thinning in both eyes (<100 μm).

Electrophysiologic assessment was performed in 25 patients at baseline (Table 2). Nine of the 25 patients (36%) were in ERG group 1 (isolated macular dysfunction), 1 (4%) was in ERG group 2, and 15 (60%) were in ERG group 3 (generalized cone and rod dysfunction).

Molecular Genetics

Detailed molecular genetic results including in silico analysis to assist in the prediction of pathogenicity of the variants are shown in Table 4 (available at www.aaojournal.org). Forty-six *ABCA4* variants were identified: 27 missense, 7 splice-site alterations,

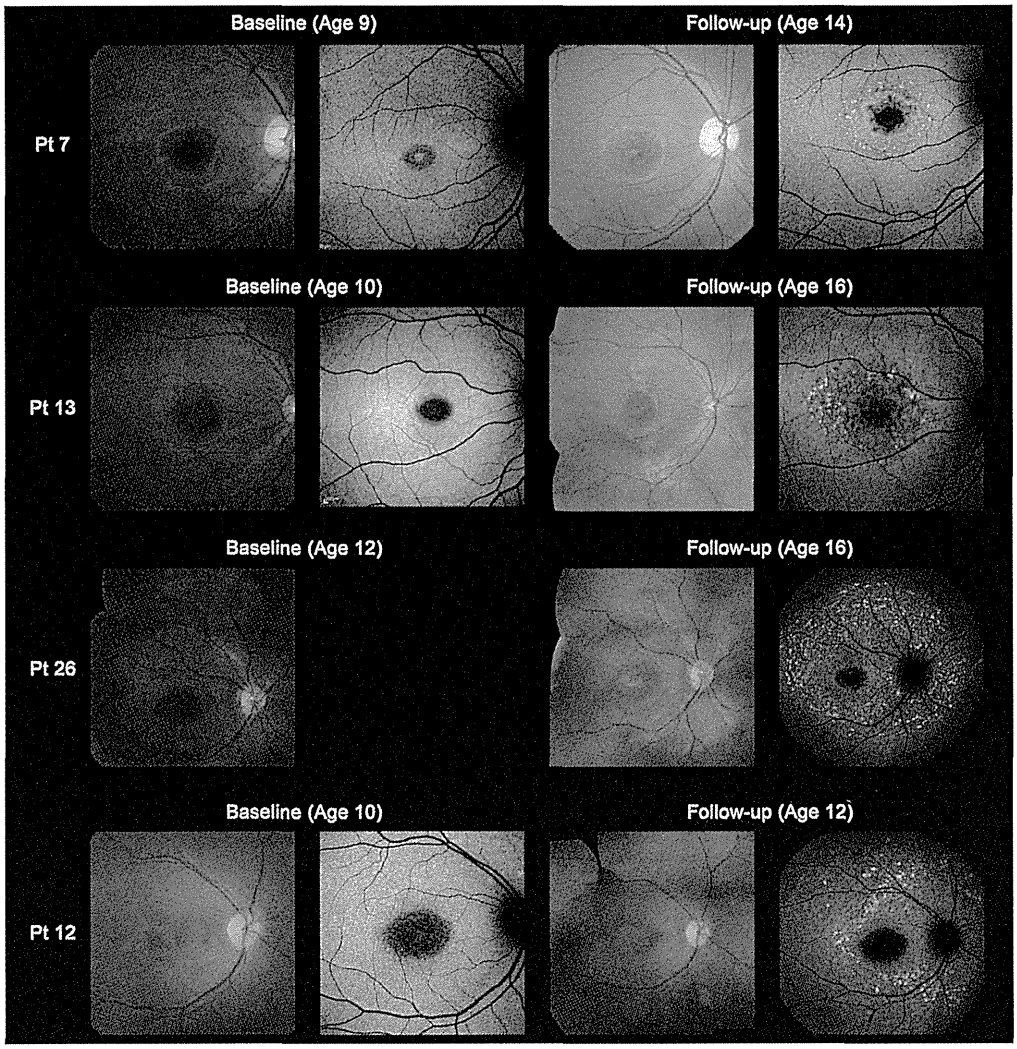

Figure 2. Color fundus photographs and autofluorescence (AF) images of 4 representative cases developing macular flecks during follow-up (patients 7, 13, 26, and 12). Color photograph of patient 7 at baseline shows subtle central atrophy without flecks (fundus grade 3a). At baseline, AF imaging demonstrates a localized low AF signal surrounded by an irregular high signal (AF type 1). Five years later, there is marked central atrophy with visible macular flecks (fundus grade 3b) and AF imaging demonstrates a localized low AF signal at the fovea with perifoveal foci of high signal (AF type 1). Patient 13 shows central atrophy with no visible flecks at baseline (fundus grade 3a), with AF imaging showing a localized low AF signal surrounded by subtle foci of high AF signal at the macula (AF type 1). Six years later, there are marked and increased macular flecks, also clearly seen on AF imaging (fundus grade 3b; AF type 1). Patient 26 has central atrophy with no visible flecks at baseline (fundus grade 3a), but marked flecks corresponding to foci of high signal on AF imaging are present 4 years later (fundus grade 3b; AF type 2). Patient 12 shows central atrophy with early subtle peripheral flecks at baseline (fundus grade 3b) and AF imaging demonstrates a localized low AF signal with subtle foci of high AF signal extending anterior to the vascular arcades (AF type 2). Two years later, there are marked and increased macular and peripheral flecks, which are also well-defined on AF imaging (fundus grade 3b; AF type 2). Pt = patient.

7 nonsense, 3 frameshifts, 1 in-frame duplication, and 1 definitely disease-associated intronic variant for which the exact pathogenic mechanism is not known. Thirteen novel definitely or highly likely disease-causing variants were identified: p.Gln8fs, p.Cys519*, p.Asp586Gly, p.Arg587Lys, p.Glu905fs, p.Tyr1027*, p.Met1066-Arg, p.Arg1097*, p.Thr1721fs, p.Tyr1770Asp, p.Ala1739dup, p.Ser2072Asn, and c.6817-2A>C (Table 4). Four homozygous variants (p.Glu905fs, p.Glu1022Lys, p.Tyr1027*, and c.6479+1G>A) were identified in patients from consanguineous families and the other 42 variants were detected in heterozygous state. Four of 8 patients from consanguineous families had homozygous variants (patients 3, 5, 6, and 28), 2 had compound heterozygous variants (patients 2 and 17), and 2 had no variants identified (patients 1 and 4).

At least 1 disease-causing *ABCA4* variant was detected in 38 of the 42 patients (90%); of these, ≥2 variants were identified in 34 (81%) and 1 variant in 4 (9.5%; Tables 2 and 4). Only 4 of the 42 individuals (9.5%) had no variants identified. The 34 patients harboring ≥2 disease-causing variants were classified based on the number and mutation type (with suggested severity) into 3 genotype subgroups: 7 patients (21%) in genotype group A, 15 (44%) in group B, and 12 (35%) in group C (Table 2).

Comparison Between Childhood-Onset and Adult-Onset STGD

Sixty-four patients with adult-onset STGD harboring ≥2 disease-causing *ABCA4* variants were reviewed. The clinical and molecular

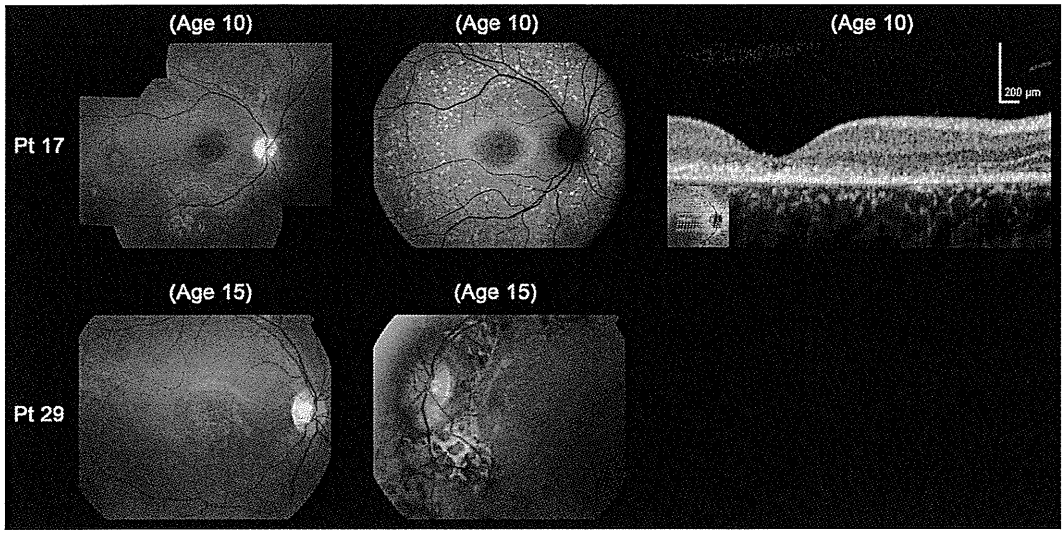

Figure 3. Color fundus photographs, autofluorescence (AF), and spectral-domain optical coherence tomographic images of 2 molecularly proven cases with "atypical" clinical features of childhood-onset Stargardt Disease (patients 17 and 29). Color photograph of patient 17 shows fine dots at the central macula surrounded by numerous peripheral flecks and AF imaging demonstrates well-defined dots associated with a high signal at the central macula surrounded by a ring of increased AF signal and numerous foci with high and low signal extending to the peripheral retina. Outer retinal loss at the macula is present on SD-OCT. Patient 29 has asymmetric fundus findings with central atrophy and peripheral flecks in the right eye and macular atrophy with flecks, subretinal fibrosis, and hyperpigmentation at the level of the retinal pigment epithelium in the left eye. Pt = patient.

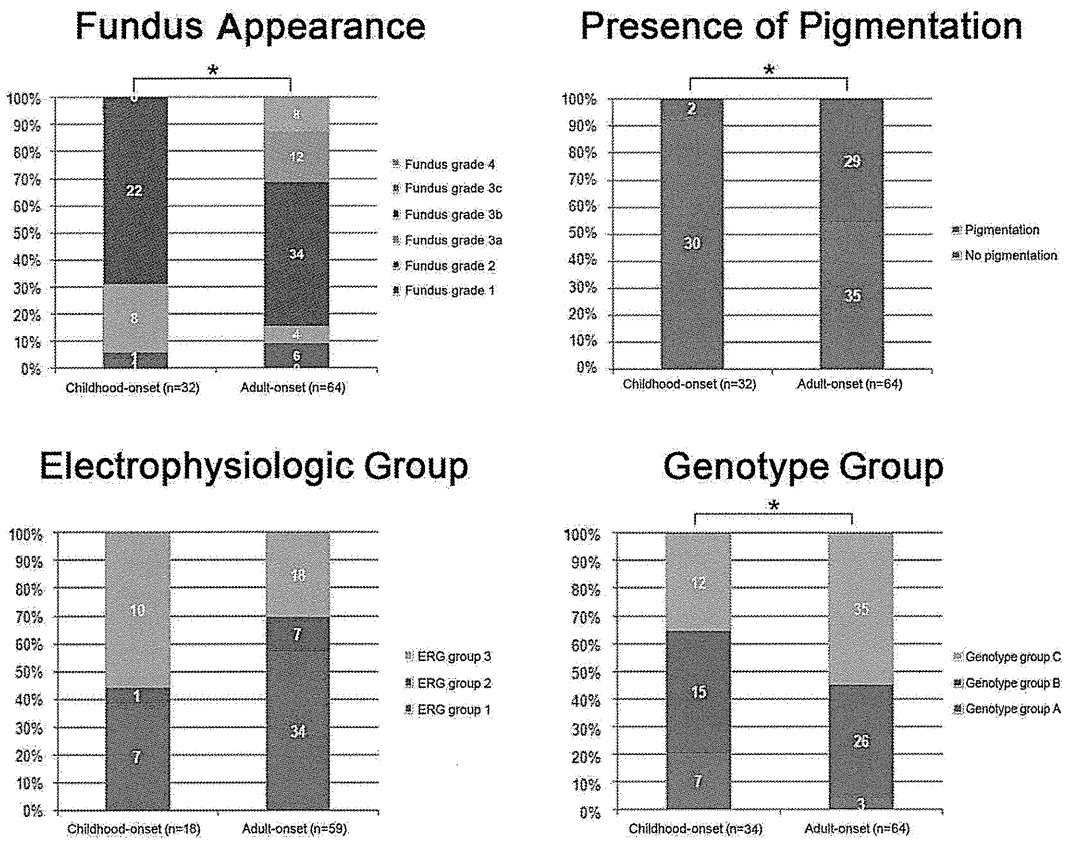

Figure 4. Comparison of the distribution of fundus appearances, presence of pigmentation, electrophysiologic group, and genotype group between a cohort with childhood-onset Stargardt disease and a group with adult-onset Stargardt disease. There are significant differences in terms of fundus appearance classification, presence of pigmentation, and genotype group classification (*$P < 0.05$). A higher proportion of patients with childhood-onset Stargardt disease are in electrophysiologic group 3 compared with adult-onset Stargardt disease, but this difference does not attain significance. ERG = electroretinography.

genetic data were compared between 34 patients with childhood-onset STGD harboring ≥2 disease-causing *ABCA4* variants and the aforementioned 64 patients with adult-onset STGD (Table 5, available at www.aaojournal.org; Fig 4).

There were significant differences in terms of fundus appearance classification (chi-square = 23.2; $P = 0.001$), presence of pigmentation (chi-square = 14.9; $P = 0.000$), genotype group classification (chi-square = 7.3; $P = 0.003$), and central foveal thickness in the selected eye ($P = 0.012$; Table 5, available at www.aaojournal.org; Figs 4 and 5, available at www.aaojournal.org); with childhood-onset STGD being associated with less retinal pigmentation, a greater proportion of patients harboring deleterious alleles, and a thinner central fovea. No differences were identified in terms of location of flecks (chi-square = 4.0; $P = 0.136$), AF pattern (chi-square = 5.6; $P = 0.061$), electrophysiologic group (chi-square = 3.8; $P = 0.148$), or logMAR VA in the selected eye ($P = 0.781$). However, a greater proportion of patients with childhood-onset STGD were in ERG group 3 (10/18; 56%) compared with adult-onset STGD (18/59 [31%]; Table 5; Fig 4), but the difference, although showing a strong trend, did not attain significance (Fig 4).

Discussion

This manuscript reports a series of childhood-onset patients with molecularly confirmed STGD, and compares the genetic, clinical, and electrophysiologic data with those in an adult-onset group.

The classical phenotype of STGD is characterized by the presence of yellowish-white fundus flecks and macular atrophy, but the fundus appearance can be variable.[1,3,12,13] Fishman described 4 groups based on fundus appearance and electrophysiologic findings[3]; the author did not distinguish between childhood-onset and adult-onset disease. In addition, the classification did not fully encompass the range of phenotypes present in childhood-onset disease and thus was modified for the present study (Table 1). Most children in this study had the classical fundus appearance of STGD with macular atrophy and macular and/or peripheral flecks, but one third of children had no visible flecks at presentation. Subsequent development of flecks was observed during the follow-up interval in 3 of these 12 patients (Fig 2). Similar development of macular/peripheral flecks over time have also been described in a young adult patient with STGD.[18]

There were no children with paracentral atrophy without central atrophy (observed in the foveal sparing phenotype, a milder phenotype seen in a minority of patients with STGD).[7,11,13,15] This observation is in keeping with previous reports that patients with a foveal sparing phenotype typically present in later adult life.[7,15] The subset with a foveal-sparing phenotype show relatively preserved foveal structure, which results in a relatively wide CFT range in the adult-onset STGD group (Fig 5).

Marked disruption of foveal outer retinal structure was present on SD-OCT in all children imaged, indicating that changes in foveal structure occur early in the disease process. Visual loss may precede ophthalmoscopic abnormalities in childhood-onset STGD and this may lead to nonorganic visual loss being considered. In such cases, SD-OCT imaging and/or electrophysiologic assessment will avoid misdiagnosis.[18] The early foveal involvement in STGD without flecks, or other AF imaging evidence of increased levels of lipofuscin in the RPE, lend support to the hypothesis that A2E, which is elevated in STGD, may be directly toxic to cone photoreceptors.[40,41]

Of the 24 patients, 9 (36%) were in ERG group 1, 1 (4%) in ERG group 2, and 15 (60%) in ERG group 3. A greater proportion of patients were in group 3 compared with the cohort with adult-onset disease, indicating that childhood-onset STGD is more likely to be associated with generalized retinal dysfunction. This is further evidence for childhood-onset STGD having a more severe retinal phenotype.[5,6,35]

Twenty-two patients (58%) had ≥1 deleterious variant and 7 subjects (18%) had 2 deleterious variants, which was significantly higher than observed in the adult-onset cohort (45% and 5%, respectively). The 5 patients (71%) with available ERGs in genotype group A (harboring 2 deleterious variants) all had generalized rod and cone system dysfunction (ERG group 3). These findings when taken together suggest that patients harboring deleterious *ABCA4* variants are more likely to have an earlier presentation (childhood) and a more severe functional phenotype.[5]

There are potential limitations of this study, including the definition of age of onset and choosing to classify childhood-onset as before the age of 17. The age of onset was defined as either the age at first symptom or the age when a retinal abnormality was first detected in "asymptomatic" patients. These 2 groups (symptomatic and asymptomatic) may have different clinical characteristics, including the symptomatic patients would be expected to have foveal involvement and thereby reduced VA. However, the vast majority of children were symptomatic in our cohort. It is also possible that dividing patients by age 17 may potentially introduce a selection bias.

This study specifically addresses, for the first time, the clinical features and molecular genetic findings of childhood-onset STGD in a substantial group of patients. Childhood-onset disease is associated with more severe VA loss from the early stages of disease. The classical flecks are not always present at diagnosis, but can appear later in the course of disease. Generalized cone and rod system dysfunction is more common than in adult-onset disease, in keeping with a more severe phenotype. Two or more disease-causing variants were detected in >80% of children and a higher proportion of definitely or possibly deleterious variants were demonstrated compared with adult-onset STGD, which is likely to underlie the earlier onset and more severe phenotype in childhood. The rapid deterioration of function in childhood-onset disease suggests that the investigation of novel therapies in this age group is more likely to lead to timely recognition of any treatment effect compared with adults with more slowly progressive disease.

Acknowledgments. The authors thank Arundhati Dev Borman, Panagiotis I. Sergouniotis, Eva Lenassi, and Yozo Miyake for data collection and insightful comments.

References

1. Michaelides M, Hunt DM, Moore AT. The genetics of inherited macular dystrophies. J Med Genet 2003;40:641–50.
2. Allikmets R, Singh N, Sun H, et al. A photoreceptor cell-specific ATP-binding transporter gene (*ABCR*) is mutated in recessive Stargardt macular dystrophy. Nat Genet 1997;15:236–46.
3. Fishman GA. Fundus flavimaculatus. A clinical classification. Arch Ophthalmol 1976;94:2061–7.
4. Michaelides M, Chen LL, Brantley MA Jr, et al. *ABCA4* mutations and discordant *ABCA4* alleles in patients and siblings with bull's-eye maculopathy. Br J Ophthalmol 2007;91:1650–5.
5. Fujinami K, Lois N, Davidson AE, et al. A longitudinal study of Stargardt disease: clinical and electrophysiologic assessment, progression, and genotype correlations. Am J Ophthalmol 2013;155:1075–88.
6. Fujinami K, Sergouniotis PI, Davidson AE, et al. The clinical effect of homozygous *ABCA4* alleles in 18 patients. Ophthalmology 2013;120:2324–31.
7. Fujinami K, Sergouniotis PI, Davidson AE, et al. Clinical and molecular analysis of Stargardt disease with preserved foveal structure and function. Am J Ophthalmol 2013;156:487–501.
8. Fujinami K, Zernant J, Chana RK, et al. *ABCA4* gene screening by next-generation sequencing in a British cohort. Invest Ophthalmol Vis Sci 2013;54:6662–74.
9. Fujinami K, Singh R, Carroll J, et al. Fine central macular dots associated with childhood-onset Stargardt Disease [letter online]. Acta Ophthalmol 2014;92:e157–9.
10. Fujianami K, Lois N, Mukherjee R, et al. A longitudinal study of Stargardt disease: quantitative assessment of fundus autofluorescence, progression and genotype correlations. Invest Ophthalmol Vis Sci 2014;54:8181–90.
11. Fujinami K, Akahori M, Fukui M, et al. Stargardt disease with preserved central vision: identification of a putative novel mutation in ATP-binding cassette transporter gene [letter online]. Acta Ophthalmol 2011;89:e297–8.
12. Burke TR, Tsang SH. Allelic and phenotypic heterogeneity in *ABCA4* mutations. Ophthalmic Genet 2011;32:165–74.
13. Rotenstreich Y, Fishman GA, Anderson RJ. Visual acuity loss and clinical observations in a large series of patients with Stargardt disease. Ophthalmology 2003;110:1151–8.
14. Wabbels B, Demmler A, Paunescu K, et al. Fundus autofluorescence in children and teenagers with hereditary retinal diseases. Graefes Arch Clin Exp Ophthalmol 2006;244:36–45.
15. Westeneng-van Haaften SC, Boon CJ, Cremers FP, et al. Clinical and genetic characteristics of late-onset Stargardt's disease. Ophthalmology 2012;119:1199–210.
16. Fishman GA, Stone EM, Grover S, et al. Variation of clinical expression in patients with Stargardt dystrophy and sequence variations in the *ABCR* gene. Arch Ophthalmol 1999;117:504–10.
17. Fumagalli A, Ferrari M, Soriani N, et al. Mutational scanning of the ABCR gene with double-gradient denaturing-gradient gel electrophoresis (DG-DGGE) in Italian Stargardt disease patients. Hum Genet 2001;109:326–38.
18. Jarc-Vidmar M, Perovsek D, Glavac D, et al. Morphology and function of the retina in children and young adults with Stargardt dystrophy. Zdrav Vestn 2012;81(suppl):I-51–60.
19. Cremers FP, van de Pol DJ, van Driel M, et al. Autosomal recessive retinitis pigmentosa and cone-rod dystrophy caused by splice site mutations in the Stargardt's disease gene *ABCR*. Hum Mol Genet 1998;7:355–62.
20. Briggs CE, Rucinski D, Rosenfeld PJ, et al. Mutations in *ABCR (ABCA4)* in patients with Stargardt macular degeneration or cone-rod degeneration. Invest Ophthalmol Vis Sci 2001;42:2229–36.
21. Allikmets R, Wasserman WW, Hutchinson A, et al. Organization of the *ABCR* gene: analysis of promoter and splice junction sequences. Gene 1998;215:111–22.
22. Zernant J, Schubert C, Im KM, et al. Analysis of the *ABCA4* gene by next-generation sequencing. Invest Ophthalmol Vis Sci 2011;52:8479–87.
23. Rozet JM, Gerber S, Souied E, et al. Spectrum of ABCR gene mutations in autosomal recessive macular dystrophies. Eur J Hum Genet 1998;6:291–5.
24. Lewis RA, Shroyer NF, Singh N, et al. Genotype/phenotype analysis of a photoreceptor-specific ATP-binding cassette transporter gene, *ABCR*, in Stargardt disease. Am J Hum Genet 1999;64:422–34.
25. Rivera A, White K, Stohr H, et al. A comprehensive survey of sequence variation in the *ABCA4 (ABCR)* gene in Stargardt disease and age-related macular degeneration. Am J Hum Genet 2000;67:800–13.
26. Webster AR, Heon E, Lotery AJ, et al. An analysis of allelic variation in the *ABCA4* gene. Invest Ophthalmol Vis Sci 2001;42:1179–89.
27. Shroyer NF, Lewis RA, Yatsenko AN, et al. Cosegregation and functional analysis of mutant *ABCR (ABCA4)* alleles in families that manifest both Stargardt disease and age-related macular degeneration. Hum Mol Genet 2001;10:2671–8.
28. Klevering BJ, Blankenagel A, Maugeri A, et al. Phenotypic spectrum of autosomal recessive cone-rod dystrophies caused by mutations in the *ABCA4 (ABCR)* gene. Invest Ophthalmol Vis Sci 2002;43:1980–5.
29. Fishman GA, Stone EM, Eliason DA, et al. *ABCA4* gene sequence variations in patients with autosomal recessive cone-rod dystrophy. Arch Ophthalmol 2003;121:851–5.
30. Simonelli F, Testa F, Zernant J, et al. Genotype-phenotype correlation in Italian families with Stargardt disease. Ophthalmic Res 2005;37:159–67.
31. Littink KW, Koenekoop RK, van den Born LI, et al. Homozygosity mapping in patients with cone-rod dystrophy: novel mutations and clinical characterizations. Invest Ophthalmol Vis Sci 2010;51:5943–51.
32. Aguirre-Lamban J, Gonzalez-Aguilera JJ, Riveiro-Alvarez R, et al. Further associations between mutations and polymorphisms in the *ABCA4* gene: clinical implication of allelic variants and their role as protector/risk factors. Invest Ophthalmol Vis Sci 2011;52:6206–12.
33. Riveiro-Alvarez R, Lopez-Martinez MA, Zernant J, et al. Outcome of *ABCA4* disease-associated alleles in autosomal recessive retinal dystrophies: retrospective analysis in 420 Spanish families. Ophthalmology 2013;120:2332–7.
34. Maugeri A, van Driel MA, van de Pol DJ, et al. The 2588G–>C mutation in the *ABCR* gene is a mild frequent founder mutation in the Western European population and allows the classification of *ABCR* mutations in patients with Stargardt disease. Am J Hum Genet 1999;64:1024–35.
35. Lois N, Holder GE, Bunce C, et al. Phenotypic subtypes of Stargardt macular dystrophy-fundus flavimaculatus. Arch Ophthalmol 2001;119:359–69.
36. McBain VA, Townend J, Lois N. Progression of retinal pigment epithelial atrophy in Stargardt disease. Am J Ophthalmol 2012;154:146–54.
37. Sergouniotis PI, Davidson AE, Lenassi E, et al. Retinal structure, function, and molecular pathologic features in gyrate atrophy. Ophthalmology 2012;119:596–605.
38. Marmor MF, Fulton AB, Holder GE, et al; International Society for Clinical Electrophysiology of Vision. ISCEV standard for full-field clinical electroretinography (2008 update). Doc Ophthalmol 2009;118:69–77.

39. Bach M, Brigell MG, Hawlina M, et al. ISCEV standard for clinical pattern electroretinography (PERG): 2012 update. Doc Ophthalmol 2013;126:1–7.
40. Mata NL, Weng J, Travis GH. Biosynthesis of a major lipofuscin fluorophore in mice and humans with *ABCR*-mediated retinal and macular degeneration. Proc Natl Acad Sci U S A 2000;97:7154–9.
41. Conley SM, Cai X, Makkia R, et al. Increased cone sensitivity to ABCA4 deficiency provides insight into macular vision loss in Stargardt's dystrophy. Biochim Biophys Acta 2012;1822:1169–79.

Footnotes and Financial Disclosures

Originally received: March 4, 2014.
Final revision: July 21, 2014.
Accepted: August 4, 2014.
Available online: October 10, 2014. Manuscript no. 2014-345.

[1] Laboratory of Visual Physiology, National Institute of Sensory Organs, National Hospital Organization, Tokyo Medical Center, Tokyo, Japan.

[2] Department of Ophthalmology, Keio University, School of Medicine, Tokyo, Japan.

[3] UCL Institute of Ophthalmology, London, UK.

[4] Moorfields Eye Hospital, City Road, London, UK.

[5] Department of Ophthalmology, Columbia University, New York, New York.

[6] Department of Pathology and Cell Biology, Columbia University, New York, New York.

*Both authors (Prof. Michaelides and Prof. Moore) are joint senior authors on this paper.

Financial Disclosure(s):
The author have no proprietary or commercial interest in any materials discussed in this article. The sponsor or funding organization had no role in the design or conduct of this research.

Supported by grants from the National Institute for Health Research Biomedical Research Center at Moorfields Eye Hospital NHS Foundation Trust and UCL Institute of Ophthalmology (UK), Foundation Fighting Blindness (USA), Fight for Sight (UK), Moorfields Eye Hospital Special Trustees (UK), Macular Disease Society (UK), National Eye Institute EY021163, EY019861, and EY019007 (Core Support for Vision Research), unrestricted funds from Research to Prevent Blindness (New York, NY) to the Department of Ophthalmology, Columbia University, Suzuken Memorial Foundation (Japan), Mitsukoshi Health and Welfare Foundation (Japan), and Daiwa Anglo-Japanese Foundation (Japan), Grant-in-Aid for Young Scientists (B) of the Ministry of Education, Culture, Sports, Science and Technology (Japan). MM is supported by a Foundation Fighting Blindness Career Development Award (USA). ATM is the Chairman of the Data Safety and Management Committee of an Oxford Biomedica sponsored clinical trial of gene replacement therapy for Stargardt disease.

Correspondence:
Professor Anthony T. Moore and Michel Michaelides, University College London, Institute of Ophthalmology, 11-43 Bath Street, London, EC1V 9EL, United Kingdom. E-mail: tony.moore@ucl.ac.uk or michel.michaelides@ucl.ac.uk

Doc Ophthalmol
DOI 10.1007/s10633-014-9464-8

CLINICAL CASE REPORT

Novel nonsense and splice site mutations in *CRB1* gene in two Japanese patients with early-onset retinal dystrophy

Kazuki Kuniyoshi · Kazuho Ikeo · Hiroyuki Sakuramoto · Masaaki Furuno · Kazutoshi Yoshitake · Yoshikazu Hatsukawa · Akira Nakao · Kazushige Tsunoda · Shunji Kusaka · Yoshikazu Shimomura · Takeshi Iwata

Received: 25 June 2014 / Accepted: 8 October 2014

Abstract
Purpose To report novel mutations in the *CRB1* gene in two patients with early-onset retinal dystrophy (EORD) and the longitudinal clinical course of EORD.
Patients and methods The patients were two unrelated Japanese children. Standard ophthalmic examinations including perimetry, electroretinography, and optical coherence tomography were performed on both patients. Whole exomes of the patients and their nonsymptomatic parents were analyzed using a next-generation sequence (NGS) technique.
Results *Patient 1* was noted to have esotropia and hyperopia at age 3. His decimal best-corrected visual acuity (BCVA) was 0.6 OD and 0.3 OS at age 6 with de-pigmentation of the retinal pigment epithelium (RPE). At age 19, his central vision was still preserved; however, numerous pigment granules were present in the retina. NGS analysis revealed a p.R632X nonsense and c.652 + 1_652 + 4delGTAA splice site mutations in the *CRB1* gene. *Patient 2* was noted to have hyperopia at age 3. His decimal BCVA at age 6 was 0.3 OD and 0.4 OS with de-pigmented RPE. The degree of retinal pigmentation was increased but his BCVA was good until the age of 14 years. NGS analysis revealed c.652 + 1_652 + 4delGTAA and c.652 + 1_652 + 2insT splice site mutations in the *CRB1* gene.
Conclusions The phenotypes of these novel mutations for EORD are typical of *CRB1*-associated EORD (LCA8). They were slowly progressive until the second decade of life.

K. Kuniyoshi (✉) · H. Sakuramoto · A. Nakao · Y. Shimomura
Department of Ophthalmology, Kinki University Faculty of Medicine, 377-2 Ohno-Higashi, Osaka-Sayama City, Osaka 589-8511, Japan
e-mail: kuniyoshi-kazuki@umin.net

K. Ikeo · K. Yoshitake
Laboratory of DNA Data Analysis, National Institute of Genetics, Shizuoka, Japan

M. Furuno
Transcriptome Technology Team, Life Science Accelerator Technology Group, Division of Genomic Technologies, RIKEN Center for Life Science Technologies, Yokohama, Japan

Y. Hatsukawa
Department of Ophthalmology, Osaka Medical Center and Research Institute for Maternal and Child Health, Osaka, Japan

K. Tsunoda
Laboratory of Visual Physiology, National Institute of Sensory Organs, National Hospital Organization Tokyo Medical Center, Tokyo, Japan

S. Kusaka
Department of Ophthalmology, Sakai Hospital, Kinki University Faculty of Medicine, Osaka, Japan

T. Iwata
Division of Molecular and Cellular Biology, National Institute of Sensory Organs, National Hospital Organization Tokyo Medical Center, Tokyo, Japan

Published online: 17 October 2014

Keywords Leber congenital amaurosis · Early-onset retinal dystrophy · *CRB1* · Optical coherence tomography · Electroretinography · Visual fields · Japanese

Introduction

The early-onset retinal dystrophies (EORDs) are a milder form of Leber congenital amaurosis (LCA) [1, 2], and EORDs and LCA are considered to be clinically similar diseases (LCA/EORD). The onset of the signs and symptoms of LCA/EORD is usually from birth through the first decade of life [1, 2]. The appearance of the fundus of eyes with LCA/EORD varies from normal, flecked retina to diffuse pigmentary retinal degeneration [3].

To date, 17 causative genes have been reported for LCA/EORD [4, 5]. Among them, the *CRB1* (crumbs homolog 1) gene, which is located on chromosome 1q31.3, was reported to be causative for LCA/EORD in 2001 (LCA8) [6]; the prevalence of LCA/EORD is estimated to be 10 % [6]. The phenotypes of *CRB1*-associated retinopathy varies from LCA/EORD [6–9], retinitis pigmentosa [10–12], paraarterior preserved retinal dystrophy [7, 9], and retinal telangiectasia with exudation (Coats-like vasculopathy) [11]. The inheritance pattern is usually autosomal recessive [6–12].

We report the clinical course and findings of genetic examinations of two unrelated Japanese patients with EORD.

Patients and methods

The patients were 2 unrelated Japanese children. Standard ophthalmic examinations including perimetry, electroretinography (ERG), and optical coherence tomography (OCT) were performed on each patient. Full-field ERGs were recorded according to the guidelines of International Society for Clinical Electrophysiology of Vision (ISCEV) [13] with a contact-lens electrode with embedded white light-emitting diodes (LEDs; EW-102; Mayo Corporation, Inazawa, Japan). The LEDs were controlled by a driver (WLS-20; Mayo Corporation, Inazawa, Japan), and the responses were amplified with a bioamplifier (MEB-5504; Nihon Kohden, Tokyo, Japan). The OCT image was obtained by Cirrus^{TM} HD-OCT version 5.1 (Carl Zeiss Meditec, Dublin, CA, USA).

Genetic investigations of the whole exome were performed with the next-generation sequencing (NGS) technique. Details of the genetic investigation have been described [14].

The research protocol was approved by the Ethics Review Board of the Kinki University Faculty of Medicine in November 2011 and conformed to the tenets of the Declaration of Helsinki of the World Medical Association. The genetic analyses were performed after obtaining a signed informed consent form from all of the parents of the patients.

Results

A summary of the clinical findings is presented in Figs. 1, 2 and 3.

Patient 1 (F64-kinki 1136)

Patient 1 was 6-year-old boy at the initial visit to our clinic. He had night blindness from his infancy and was noted to have esotropia at age 3. His parents were nonconsanguineous. His decimal best-corrected visual acuity (BCVA) at age 6 was 0.5 with +5.0 diopters sphere (DS) OD and 0.3 with +7.0 DS OS. The refractive errors were obtained with cycloplegia. He had no nystagmus. Ophthalmoscopy revealed de-pigmentation of the retinal pigment epithelium (RPE) in the mid-periphery (Fig. 1). The ERGs were reduced, and perimetry revealed scotomas in the mid-periphery (Figs. 1, 3). He was observed for 13 years, and his BCVA at age 19 was 0.8 OD and 0.1 OS. During the follow-up period, numerous clumped pigments appeared in the mid-periphery of the retina (Fig. 1). The scotomas gradually enlarged but the ERGs decreased only slightly (Figs. 1, 3). OCT revealed a thickened and disorganized retina in both eyes (Fig. 1).

NGS on his whole exome revealed 1,650,353 mutations when compared with the reference human genome. Among them, 455 mutations were selected which could change the amino acid sequence after an exclusion of common mutations. They were filtered, and 7 genes were selected as causal candidates. Finally, *CRB1* was selected to be the disease-causing gene because the other genes

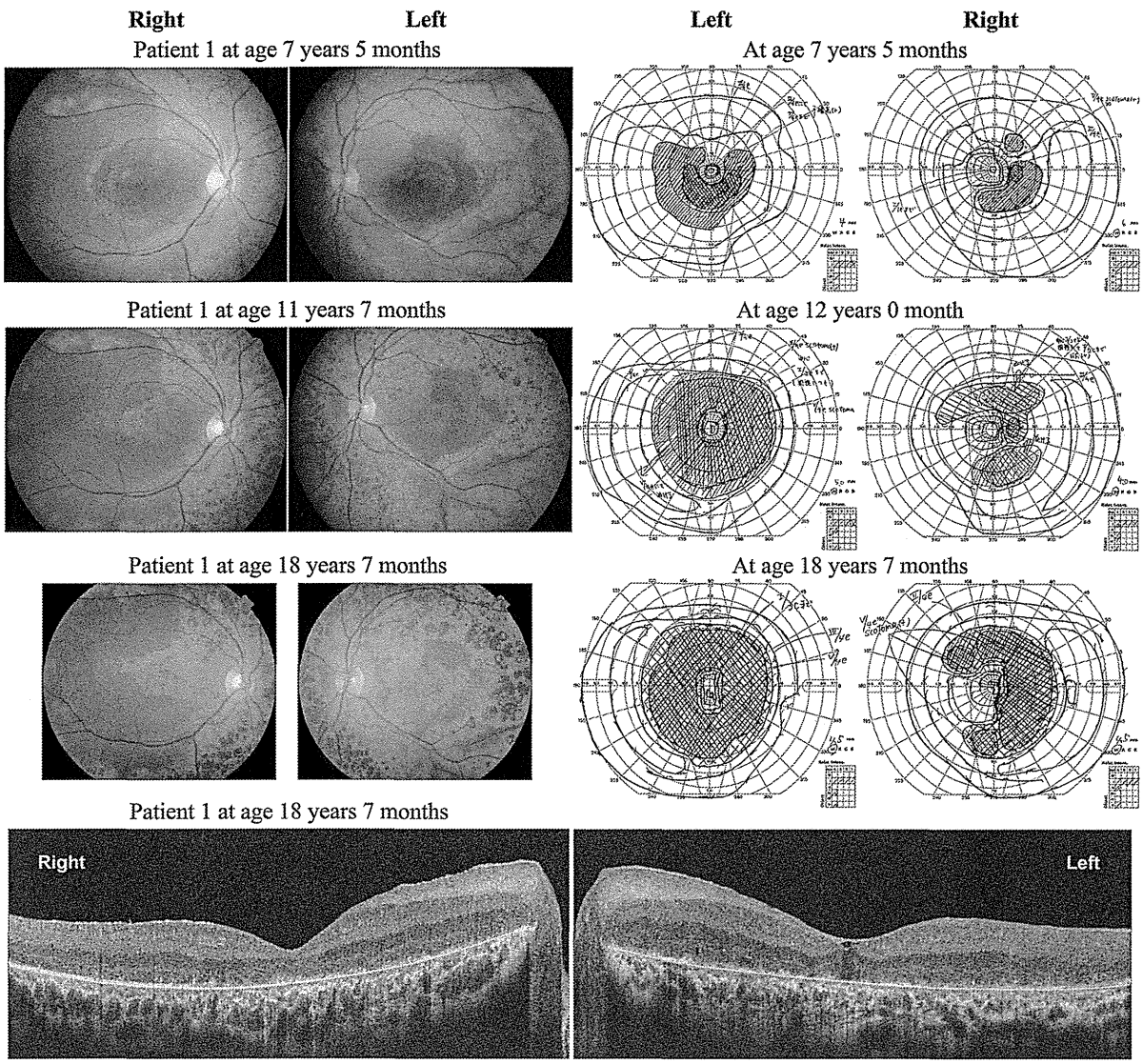

Fig. 1 Fundus photographs (*left column*), Goldmann kinetic visual fields (*right column*), and *horizontal* section of optical coherence tomographic (OCT) image (*bottom*) of Patient 1. The fundi of the two eyes show a preservation of the para-arteriolar retinal pigment epithelium (RPE). During the follow-up period, numerous clumps of pigments appeared in the mid-periphery and *yellowish* mottling of the macula became gradually apparent (*left column*). The OCT images revealed thickened and disorganized retinae (*bottom*). Length of the OCT scanning is 9 mm

were not registered in the RetNet™ database [4] as causative for inherited retinal diseases.

Genetic analysis revealed compound heterozygous mutations, p.R632X nonsense mutation, and c.652 + 1_652 + 4delGTAA splice site mutation in the *CRB1* gene. Genetic analysis of his father revealed heterozygous p.R632X nonsense mutation and that of his mother revealed heterozygous c.652 + 1_652 + 4delGTAA splice site mutation.

Patient 2 (F84-kinki 1194)

Patient 2 was a 6-year-old boy from a family unrelated to Patient 1. He had night blindness from his infancy and was noted to be hyperopic at age 3. His parents were nonconsanguineous. His BCVA at age 6 was 0.3 OD and 0.3 OS. His cycloplegic refractive errors were +3.0 DS and −1.5 D cylinder (DC) ax180° in the right eye and +3.75 DS and −2.5 DC ax180° in the left eye.

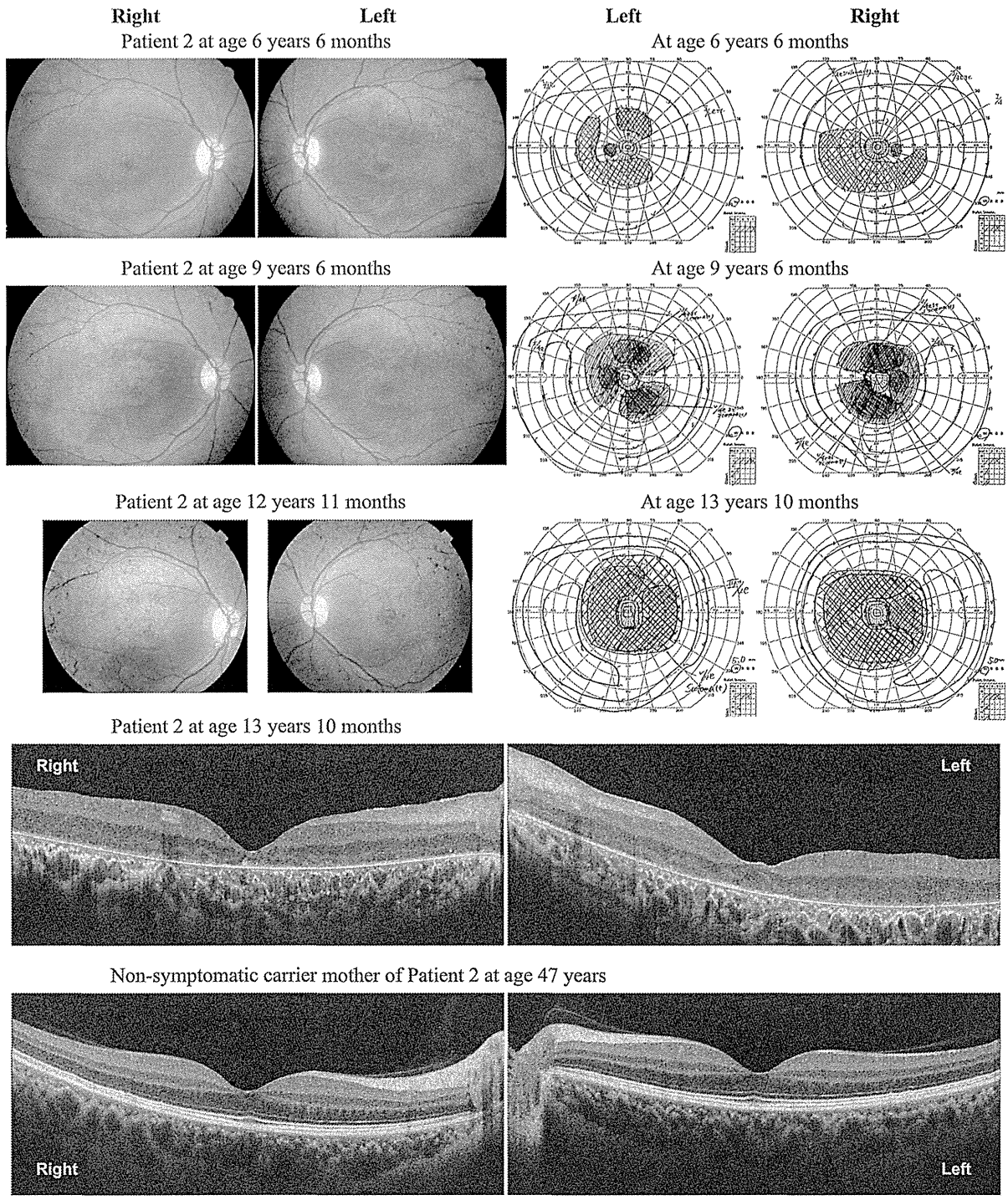

Fig. 2 Fundus photographs (*left column*), Goldmann kinetic visual fields (*right column*), and *horizontal* section of OCT image (*lower*) in Patient 2. The phenotype and clinical course are similar to those in Patient 1; however, Patient 2 has bone-spicule pigmentation. The OCT images of nonsymptomatic carrier mother are presented at the *bottom*; they are normally laminated. Length of the OCT scanning is 9 mm

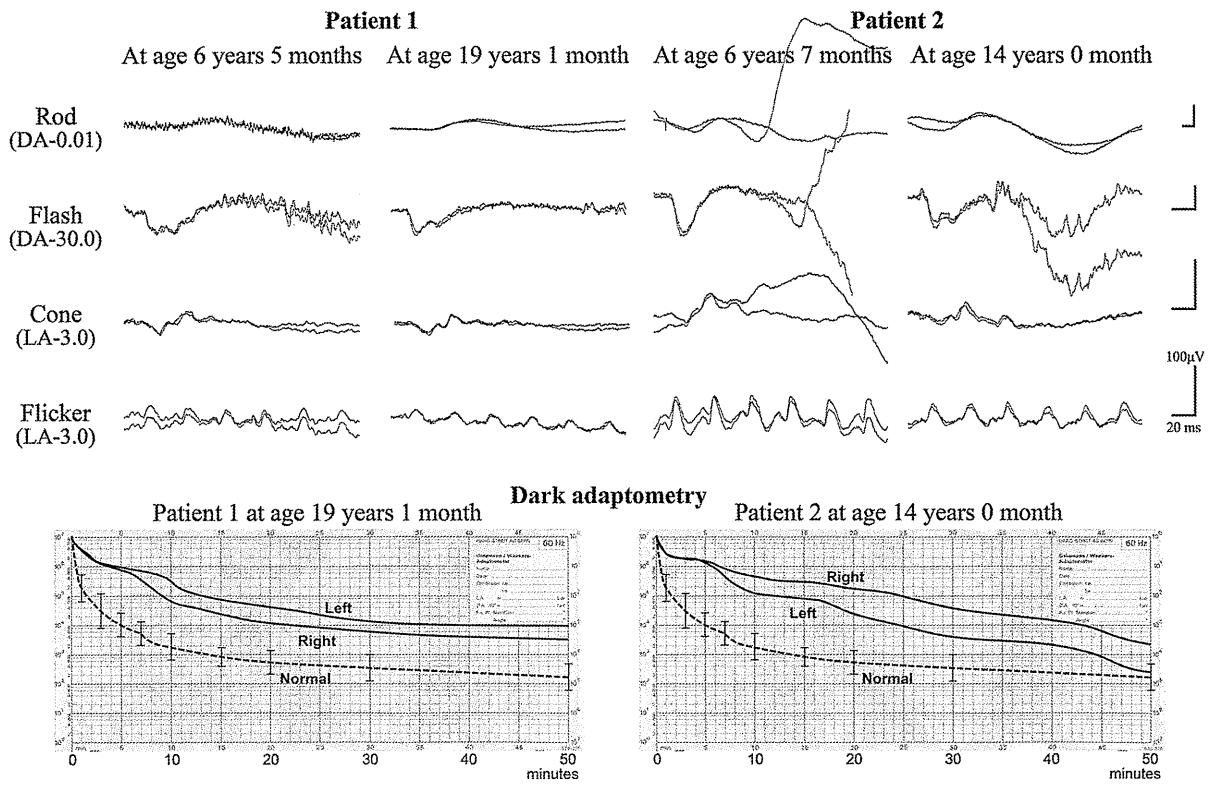

Fig. 3 Results of full-field electroretinography (ERG) (*upper*) and dark adaptometry (*lower*) in Patients 1 and 2. ERG responses from both eyes are superimposed. ERGs were not reduced much during the clinical follow-up. *Dashed lines* and *vertical bars* are the means ± standard deviations of normal controls. *DA* dark-adapted, *LA* light-adapted

He had no nystagmus. His phenotype and clinical course were similar to those in Patient 1; however, Patient 2 had bone-spicule pigmentation (Figs. 2, 3). He was observed for 8 years, and his BCVA at age 14 was 0.3 OD and 0.4 OS.

NGS analysis on his whole exome revealed 1,555,508 mutations compared with the reference human genome. Among them, 447 mutations remained as candidates after exclusion of common mutations. They were filtered, and six genes were selected as causal candidates. Finally, *CRB1* was selected as causative for his disease because the other genes were not registered in the RetNet^{TM} database [4].

Thus, genetic analysis revealed compound heterozygous mutations and c.652 + 1_652 + 4delGTAA and c.652 + 1_652 + 2insT splice site mutations in the *CRB1* gene. Genetic analysis of his father revealed heterozygous c.652 + 1_652 + 4delGTAA and that of his mother revealed heterozygous c.652 + 1_652 + 2insT splice site mutation. It was confirmed that his brother who had normal eyesight did not have these mutations.

Discussion

The three mutations in our patients, namely the p.R632X nonsense mutation, and the c.652 + 1_652 + 4delGTAA and c.652 + 1_652 + 2insT splice site mutations in the *CRB1* gene have not been reported as causative for retinal dystrophy. The first nonsense mutation is located in exon 6, and the latter two splice site mutations are in exon 2 of the 12 exons in the *CRB1* gene [15]. Thus, the first nonsense mutation truncates the protein to approximately one-half, and the latter two splice site mutations truncate the protein to 1/5 of the original size. Thus, they will lead to a loss of almost the entire molecule of the CRB1 protein.

Against expectations from these mutations, the phenotypes of our patients were not severe. They did

not have nystagmus, and they had relatively good daytime vision until the second decade of life. ERGs were recordable until the ages of 19 and 14 years (Fig. 3), and amplitudes were comparable to those reported [9]. These findings suggest that other unknown factors may influence the severity and variation of the phenotype of the *CRB1*-associated retinopathy [6–12].

A thickened and coarsely laminated retina was seen in the OCT images (Figs. 1, 2), which is characteristic of *CRB1*-associated retinopathy [9, 16]. This OCT finding is very similar to that reported by Jacobson et al. [16]. They reported that the disorganized retina was similar to an immature normal retina, and the disorganization resulted from an abnormal development caused by nonfunctioning CRB1 protein. The CRB1 protein plays a role in the polarity of the photoreceptor cells during retinal development [15]. The OCT image in the carrier mother of Patient 2, who had a heterozygous splice site mutation in exon 2 of the *CRB1* gene, had normal lamination (Fig. 2).

In conclusion, we report three novel mutations in patients with EORD, who had typical phenotypes of *CRB1*-associated EORD. Although the progression of their retinal dysfunction was slow, more longitudinal observations are needed because Henderson et al. [9] reported that vision in *CRB1*-associated patients declined to counting finger or worse in their thirties.

Acknowledgments This research was supported by the research Grants to T.I., K.T., Y.S., and K.K. from the Ministry of Health, Labour and Welfare, Japan (13803661, 23164001, and 82259921), to S.K. and K.K. from Japan Society for the Promotion of Science, Japan (23592597), and to M.F. from the Japanese Ministry of Education, Culture, Sports, Science and Technology (MEXT) for RIKEN Center for Life Science Technologies.

References

1. Leber T (1869) Ueber Retinitis pigmentosa und angeborene Amaurose. Graefes Arch Klin Exp Ophthalmol 15:1–25
2. Leber T (1916) Die Pigmentdegeneration der Netzhaut und die mit ihr verwandten Erkrankungen. In: Saemisch T, Elschnig A (eds) Graefe-Saemisch-Hess Handbuch der gesamten Augenheilkunde. Verlag von Wilherm Engelmann, Leipzig, Zweite Hälfte, pp 1076–1225
3. Weleber RG, Gregory-Evans K (2006) Leber congenital amaurosis. In: Hinton DR (ed), Ryan SJ (ed in chief) Retina, 4th edn, vol. 1. Elsevier, Philadelphia, pp 455–457
4. Daiger SP, The University of Texas Health Science Center (2014) RetNet™. Retinal information network. Updated September 11, 2014. https://sph.uth.edu/retnet/. Accessed 30 Sept 2014
5. Weleber RG, Francis PJ, Trzupek KM, Beattie C (2013) Leber congenital amaurosis. In: Pagon RA (ed in chief). GeneReviews®. NCBI Bookshelf. http://www.ncbi.nlm.nih.gov/books/NBK1298/. Accessed 30 Sept 2014
6. Lotery AJ, Jacobson SG, Fishman GA, Weleber RG, Fulton AB, Namperumalsamy P, Héon E, Levin AV, Grover S, Rosenow JR, Kopp KK, Sheffield VC, Stone EM (2001) Mutations in the *CRB1* gene cause Leber congenital amaurosis. Arch Ophthalmol 119:415–420
7. den Hollander Al, Davis J, van der Velde-Visser SD, Zonneveld MN, Pierrottet CO, Koenekoop RK, Kellner U, van den Born LI, Heckenlively JR, Hoyng CB, Handford PA, Roepman R, Cremers FPM (2004) CRB1 mutation spectrum in inherited retinal dystrophies. Hum Mutat 24:355–369
8. Hanein S, Perrault I, Gerber S, Tanguy G, Barbet F, Ducroq D, Calvas P, Dollfus H, Hamel C, Lopponen T, Munier F, Santos L, Shalev S, Zafeiriou D, Dufier JL, Munnich A, Rozet JM, Kaplan J (2004) Leber congenital amaurosis: comprehensive survey of the genetic heterogeneity, refinement of the clinical definition, and genotype-phenotype correlations as a strategy for molecular diagnosis. Hum Mutat 23:306–317
9. Henderson RH, Mackay DS, Li Z, Moradi P, Sergouniotis P, Russell-Eggitt I, Thompson DA, Robson AG, Holder GE, Webster AR, Moore AT (2011) Phenotypic variability in patients with retinal dystrophies due to mutations in *CRB1*. Br J Ophthalmol 95:811–817
10. den Hollander AI, ten Brink JB, de Kok YJM, van Soest S, van den Born LI, van Driel MA, van de Pol DJR, Payne AM, Bhattacharya SS, Kellner U, Hoyng CB, Westerveld A, Brunner HG, Bleeker-Wagemakers EM, Deutman AF, Heckenlively JR, Cremers FPM, Bergen AAB (1999) Mutations in a human homologue of *Drosophila crumbs* cause retinitis pigmentosa (RP12). Nat Genet 23:217–221
11. den Hollander AI, Heckenlively JR, van den Born LI, de Kok YJM, van der Velde-Visser SD, Kellner U, Jurklies B, van Schooneveld MJ, Blankenagel A, Rohrschneider K, Wissinger B, Cruysberg JRM, Deutman AF, Brunner HG, Apfelstedt-Sylla E, Hoyng CB, Cremers FPM (2001) Leber congenital amaurosis and retinitis pigmentosa with Coats-like exudative vasculopathy are associated with mutations in the crumbs homologue 1 (*CRB1*) gene. Am J Hum Genet 69:198–203
12. Bernal S, Calaf M, Garcia-Hoyos M, Garcia-Sandoval B, Rosell J, Adan A, Ayuso C, Baiget M (2003) Study of the involvement of the *RGR*, *CRPB1*, and *CRB1* genes in the pathogenesis of autosomal recessive retinitis pigmentosa. J Med Genet 40:e89
13. Marmor MF, Fulton AB, Holder GE, Miyake Y, Brigell M, Bach M (2009) ISCEV Standard for full-field clinical electroretinography (2008 update). Doc Ophthalmol 118:69–77
14. Kuniyoshi K, Sakuramoto H, Yoshitake K, Abe K, Ikeo K, Furuno M, Tsunoda K, Kusaka S, Shimomura Y, Iwata T (2014) Longitudinal clinical course of three Japanese patients with Leber congenital amaurosis/early-onset retinal dystrophy with *RDH12* mutation. Doc Ophthalmol 128:219–228

15. Pellikka M, Tanentzapf G, Pinto M, Smith C, McGlade CJ, Ready DF, Tepass U (2002) Crumbs, the *Drosophila* homologue of human CRB1/RP12, is essential for photoreceptor morphogenesis. Nature 416:143–149
16. Jacobson SG, Cideciyan AV, Aleman TS, Pianta MJ, Sumaroka A, Schwartz SB, Smilko EE, Milam AH, Sheffield VC, Stone EM (2003) *Crumbs homolog 1 (CRB1)* mutations result in a thick human retina with abnormal lamination. Hum Mol Genet 12:1073–1078

Whole Exome Analysis Identifies Frequent *CNGA1* Mutations in Japanese Population with Autosomal Recessive Retinitis Pigmentosa

Satoshi Katagiri[1,2], Masakazu Akahori[1], Yuri Sergeev[3], Kazutoshi Yoshitake[4], Kazuho Ikeo[4], Masaaki Furuno[5], Takaaki Hayashi[2], Mineo Kondo[6], Shinji Ueno[7], Kazushige Tsunoda[8], Kei Shinoda[9], Kazuki Kuniyoshi[10], Yohinori Tsurusaki[11], Naomichi Matsumoto[11], Hiroshi Tsuneoka[2], Takeshi Iwata[1]*

1 Division of Molecular and Cellular Biology, National Institute of Sensory Organs, National Hospital Organization Tokyo Medical Center, Tokyo, Japan, **2** Department of Ophthalmology, The Jikei University School of Medicine, Tokyo, Japan, **3** National Eye Institute, National Institutes of Health, Bethesda, MD, United States of America, **4** Laboratory of DNA Data Analysis, National Institute of Genetics, Shizuoka, Japan, **5** RIKEN Center for Life Science Technologies, Division of Genomic Technologies, Life Science Accelerator Technology Group, Transcriptome Technology Team, Yokohama, Japan, **6** Department of Ophthalmology, Mie University Graduate School of Medicine, Tsu, Japan, **7** Department of Ophthalmology, Nagoya University Graduate School of Medicine, Nagoya, Japan, **8** Laboratory of Visual Physiology, National Institute of Sensory Organs, Tokyo, Japan, **9** Department of Ophthalmology, Teikyo University School of Medicine, Tokyo, Japan, **10** Department of Ophthalmology, Kinki University Faculty of Medicine, Osaka, Japan, **11** Department of Human Genetics, Yokohama City University, Yokohama, Japan

Abstract

Objective: The purpose of this study was to investigate frequent disease-causing gene mutations in autosomal recessive retinitis pigmentosa (arRP) in the Japanese population.

Methods: In total, 99 Japanese patients with non-syndromic and unrelated arRP or sporadic RP (spRP) were recruited in this study and ophthalmic examinations were conducted for the diagnosis of RP. Among these patients, whole exome sequencing analysis of 30 RP patients and direct sequencing screening of all *CNGA1* exons of the other 69 RP patients were performed.

Results: Whole exome sequencing of 30 arRP/spRP patients identified disease-causing gene mutations of *CNGA1* (four patients), *EYS* (three patients) and *SAG* (one patient) in eight patients and potential disease-causing gene variants of *USH2A* (two patients), *EYS* (one patient), *TULP1* (one patient) and *C2orf71* (one patient) in five patients. Screening of an additional 69 arRP/spRP patients for the *CNGA1* gene mutation revealed one patient with a homozygous mutation.

Conclusions: This is the first identification of *CNGA1* mutations in arRP Japanese patients. The frequency of *CNGA1* gene mutation was 5.1% (5/99 patients). *CNGA1* mutations are one of the most frequent arRP-causing mutations in Japanese patients.

Citation: Katagiri S, Akahori M, Sergeev Y, Yoshitake K, Ikeo K, et al. (2014) Whole Exome Analysis Identifies Frequent *CNGA1* Mutations in Japanese Population with Autosomal Recessive Retinitis Pigmentosa. PLoS ONE 9(9): e108721. doi:10.1371/journal.pone.0108721

Editor: Namik Kaya, King Faisal Specialist Hospital and Research center, Saudi Arabia

Received March 4, 2014; **Accepted** August 31, 2014; **Published** September 30, 2014

Data Availability: The authors confirm that all data underlying the findings are fully available without restriction. All data are included within the manuscript and its Supporting Information files.

Funding: This study was supported by the grants to T.I. from the Ministry of Health, Labor, and Welfare of Japan (13803661); to M.A. and T.H. from the Ministry of Education, Culture, Sports, Science, and Technology of Japan (Grant-in-Aid for Scientific Research C, 25462744 and 25462738); to T.H. from the Vehicle Racing Commemorative Foundation; and to M.F. from the Research Grant for RIKEN Omics Science Center MEXT. The funders had no role in study design, data collection and analysis, decision to publish, or preparation of the manuscript.

Competing Interests: The authors have declared that no competing interests exist.

* Email: iwatatakeshi@kankakuki.go.jp

Introduction

Retinitis pigmentosa (RP; OMIM #268000) is a heterogeneous group of inherited disorders characterized by visual field loss, night blindness, abnormal color vision and fundus degeneration. The prevalence of RP is approximately 1 per 4,000 persons and more than 1 million individuals are affected worldwide [1]. The inheritance of RP shows various patterns including autosomal recessive (arRP), autosomal dominant, X-linked, sporadic (spRP), mitochondrial [2] and digenic [3] inheritance. Among the various patterns of RP inheritance, arRP is the most frequent inheritance pattern and accounts for approximately 50% to 60% of all RP patients [1]. To date, 42 arRP-causing genes and three loci have been reported in the Retinal Information Network (RetNet; https://sph.uth.edu/retnet/). Among these arRP-causing genes, mutations in Usher syndrome 2A (*USH2A*) are the most frequent and account for approximately 17% cases including cases with additional hearing loss [1]. In non-syndromic arRP, the most frequent arRP genes are eyes shut homolog (*EYS*), *USH2A* and ATP-binding cassette sub-family A member 4 (*ABCA4*), which

Table 1. Autosomal recessive retinitis pigmentosa (arRP)-causing mutations and potential arRP-causing variants found by exome sequencing.

Family ID	Gene Name	GenBank ID	Exon	Nucleotide Change	Amino Acid Change	State	Frequency*	SNP ID	Reference	Pathogenicity
RP#002	*CNGA1*	NM_000087	5	c.191delG	p.G64VfsX29	Homo	2		HGVB	Disease-causing
RP#004	*EYS*	NM_001142800	33	c.6714delT	p.P2238PfsX16	Hetero	0		Collin et al. 2008	Disease-causing
	EYS	NM_001142800	35	c.C7002A	p.C2334X	Hetero	0		This study	
RP#014	*EYS*	NM_001142800	4	c.A141T	p.E47D	Hetero	0		This study	Potential disease-causing
	EYS	NM_001142800	26	c.4957dupA	p.S1653KfsX2	Hetero	2		Iwanami et al. 2012	
RP#016	*TULP1*	NM_003322	1	c.G3A	p.M1I	Hetero	0		This study	Potential disease-causing
	TULP1	NM_003322	13	c.C1246T	p.R416C	Hetero	0	rs200769197	dbSNP	
RP#017	*EYS*	NM_001142800	26	c.4022delC	p.S1341FfsX11	Hetero	0		This study	Disease-causing
	EYS	NM_001142800	26	c.4957dupA	p.S1653KfsX2	Hetero	2		Iwanami et al. 2012	
RP#019	*CNGA1*	NM_000087	6	c.265delC	p.L89FfsX4	Hetero	2		Chen et al. 2013	Disease-causing
	CNGA1	NM_000087	11	c.1429delG	p.V477YfsX17	Hetero	0		This study	
RP#021	*CNGA1*	NM_000087	5	c.191delG	p.G64VfsX29	Homo	2		HGVB	Disease-causing
RP#023	*USH2A*	NM_206933	49	c.C9676T	p.R3226X	Hetero	0		This study	Potential disease-causing
	USH2A	NM_206933	55	c.T10859C	p.I3620T	Hetero	0		HGVB	
RP#026	*EYS*	NM_001142800	26	c.4957dupA	p.S1653KfsX2	Homo	2		Iwanami et al. 2012	Disease-causing
RP#027	*SAG*	NM_000541	11	c.926delA	p.T309TfsX12	Homo	6		Fuchs et al. 1995	Disease-causing
RP#028	*USH2A*	NM_206933	41	c.T7880C	p.I2627T	Hetero	0		This study	Potential disease-causing
	USH2A	NM_206933	55	c.C10931T	p.T3644M	Homo	1	rs185823130	dbSNP	
	USH2A	NM_206933	70	c.T15178C	p.S5060P	Hetero	0		This study	
RP#029	*CNGA1*	NM_000087	6	c.265delC	p.L89FfsX4	Homo	2		Chen et al. 2013	Disease-causing
RP#030	*C2orf71*	NM_001029883	1	c.C85T	p.R29W	Hetero	4	rs201706430	dbSNP	Potential disease-causing
	C2orf71	NM_001029883	2	c.C3748T	p.R1250C	Hetero	0		This study	

HGVB = Human Genetic Variation Browser (http://www.genome.med.kyoto-u.ac.jp/SnpDB/about.html); dbSNP = (http://www.ncbi.nlm.nih.gov/SNP/); Frequency* show the number of mutations or variants found in 1150 alleles of 575 controls.

doi:10.1371/journal.pone.0108721.t001

account for approximately 10%, 8% and 5% to 6% of cases, respectively [1,4–10].

Large scale screening of selective exons in 30 RP-causing genes was previously performed in 193 Japanese RP families [11]. Although it only targeted exons with known mutations, the study failed to identify high frequency RP genes [11]. Another study of the Japanese RP population focused on the RP genes *RHO* [12–14] and *EYS* [15,16], and found that *EYS* was a frequent arRP gene with a prevalence rate of 9% to 16% [15,16]. However, almost all reported *EYS* gene mutations in these studies have not been reported in Western populations suggesting that Japanese individuals have a different genetic background [15,16]. These results suggest that the genetic background of RP in the Japanese population is different from that in the Western population.

The recent technological development of exon capture with 99% coverage of all exons and its combination with next generation sequencing enables effective genetic studies for hereditary diseases [17–20] and the investigation of novel mutations in multiple candidate genes [21].

The purpose of this study was to find frequent arRP genes in the Japanese population. In this study, we performed whole exome analysis of 30 Japanese arRP/spRP patients with confirmation in an additional 69 arRP/spRP patients. We found frequent arRP-causing mutations in the cyclic nucleotide gated channel alpha 1 (*CNGA1*) gene.

Materials and Methods

Informed consent

The protocol of this study was approved by the Institutional Review Board at the six participating institutions (National Hospital Organization Tokyo Medical Center, Jikei University School of Medicine, Mie University School of Medicine, Nagoya University Graduate School of Medicine, Teikyo University

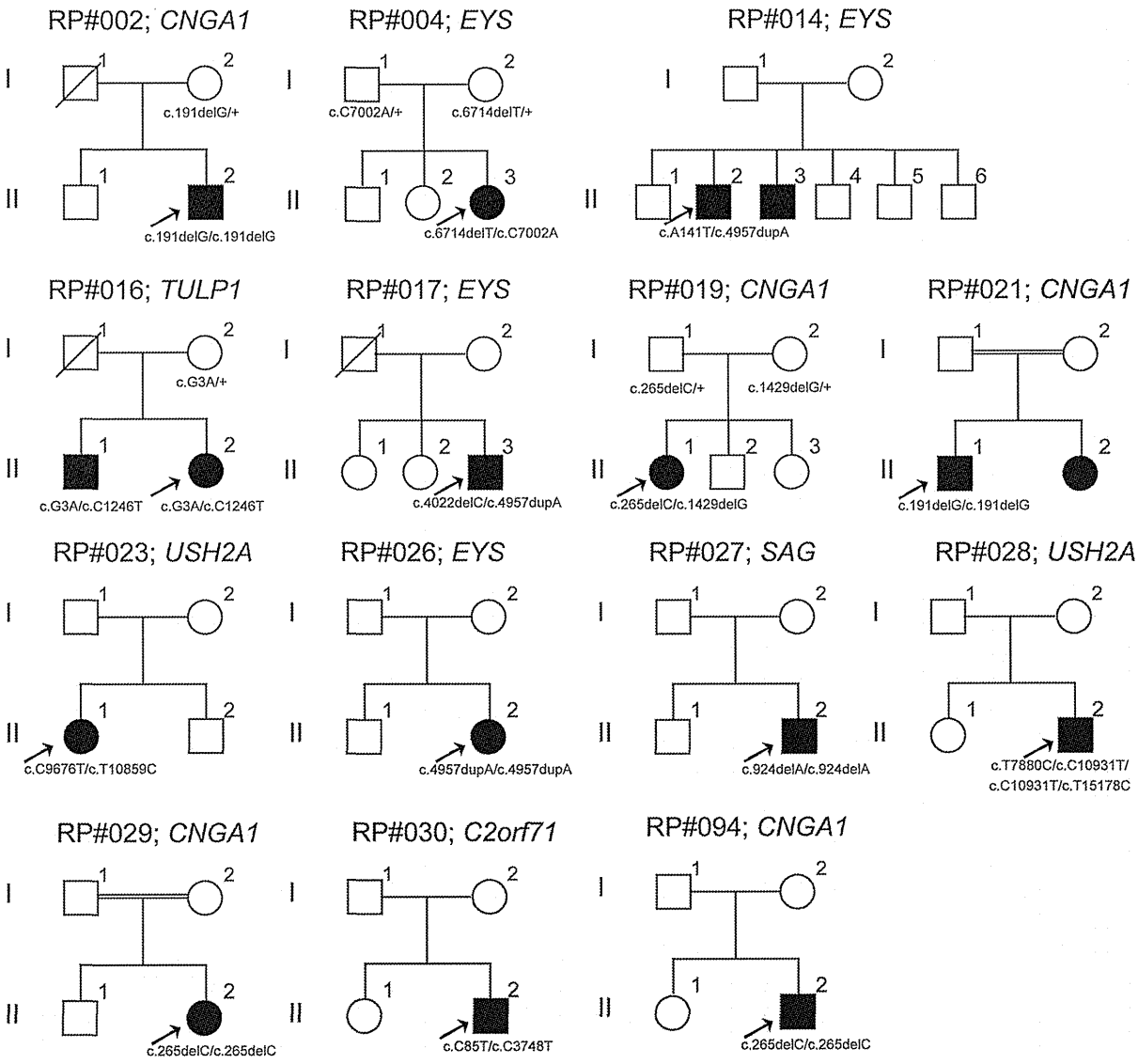

Figure 1. Pedigrees identified with arRP-causing mutations or potential arRP-causing variants. The solid squares (male) and circles (female) represent affected patients. The proband of each family is indicated by a black arrow. Unaffected family members are represented by white icons. The slash symbol indicates deceased individuals. The doubled line indicates consanguineous marriage. The generation number is shown on the left.

doi:10.1371/journal.pone.0108721.g001

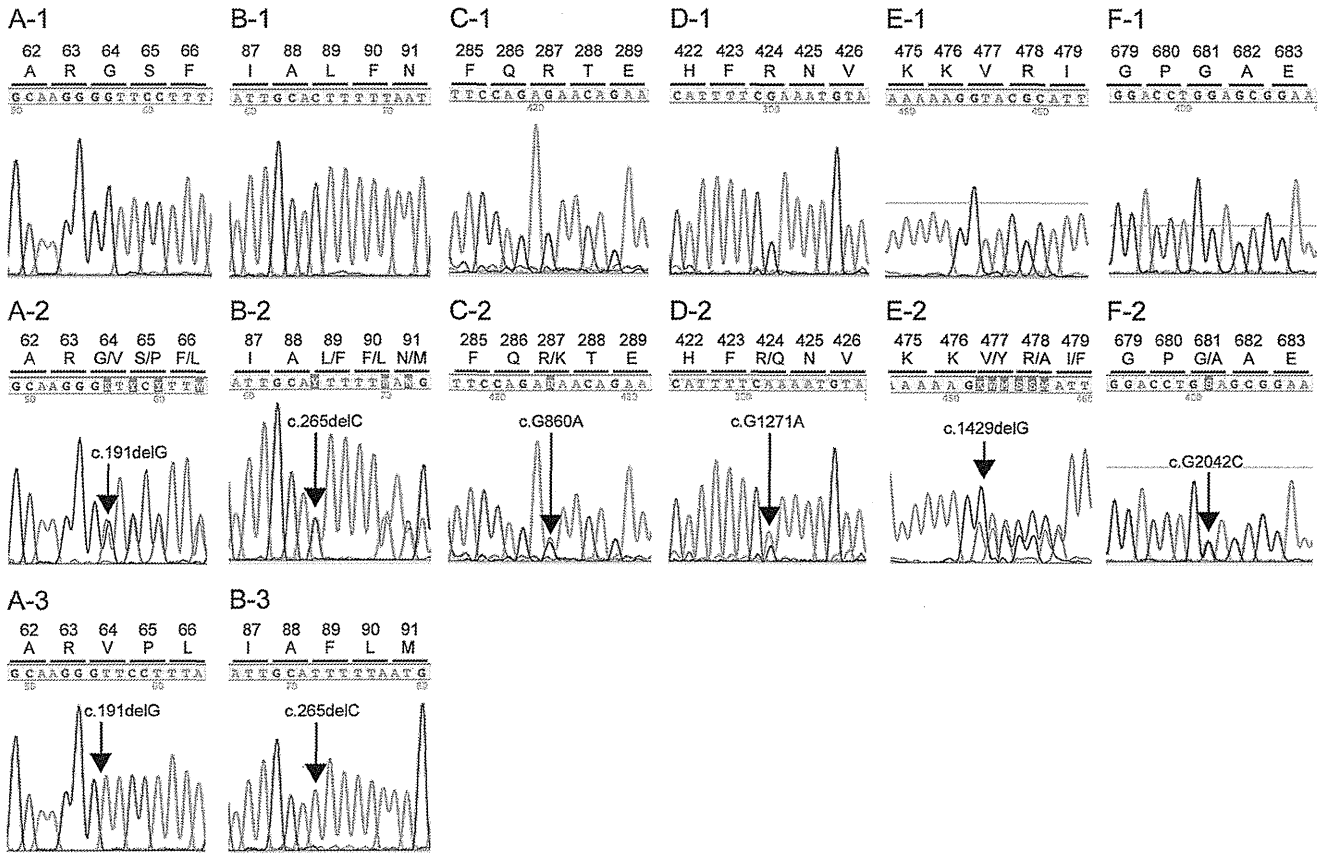

Figure 2. Sequence data of all six identified *CNGA1* mutations in this study. A-1 to F-1 show the normal sequence data for the *CNGA1* gene. A-2 to F-2 show the sequence data for heterozygous *CNGA1* mutations (c.191delG, c.265delC, c.G860A, c.G1271A, c.1429delG and c.G2042C, respectively). A-3 and B-3 show the sequence data for homozygous *CNGA1* mutations (c.191delG and c.265delC).
doi:10.1371/journal.pone.0108721.g002

School of Medicine and Kinki University Faculty of Medicine). The protocol adhered to the tenets of the Declaration of Helsinki, and signed informed consent was obtained from all participants.

Clinical studies

In total, 99 unrelated arRP/spRP patients with no apparent syndrome were recruited from the National Hospital Organization Tokyo Medical Center, Jikei University School of Medicine, Mie University School of Medicine, Nagoya University Graduate School of Medicine, Teikyo University School of Medicine and Kinki University Faculty of Medicine. The patient history was taken and ophthalmic examinations were performed. Clinical diagnosis and evaluation for RP were based on the decimal best-corrected visual acuity (BCVA), slit-lamp examination, fundus examination, visual fields determined using kinetic perimetry (Goldmann perimeter [GP]; Haag Streit, Bern, Switzerland) and electroretinography (ERG) findings. Characteristic findings for diagnosis of RP include progressive visual field loss from peripheral, night blindness, abnormal color vision, fundus degeneration represented by bone spicule pigmentations and attenuation of retinal vessels, and the more or equally decreased rod responses compared with cone responses of ERG [1,22].

DNA preparation and exome sequencing analysis

We obtained venous blood samples from all participants and genomic DNA was extracted. Whole exome sequencing was performed for 30 arRP/spRP patients using a method previously described [23]. Briefly, construction of paired-end sequence libraries and exome capture were performed by using the Agilent Bravo automated liquid-handling platform with SureSelect XT Human All Exon kit V4+ UTRs kit (Agilent Technologies, Santa Clara, CA). Enriched libraries were sequenced by using an Illumina HiSeq2000 sequencer. Reads were mapped to the reference human genome (1000 genomes phase 2 reference, hs37d5) with Burrows–Wheeler Aligner software version 0.6.2 [24]. Duplicated reads were then removed by Picard Mark Duplicates module version 1.62, and mapped reads around insertion/deletion polymorphisms were realigned by using the Genome Analysis Toolkit (GATK) version 2.1–13 [25]. Base-quality scores were recalibrated by using GATK. To extract potentially RP-causing variants, we focused only on variants that could change the amino acid sequence, such as non-synonymous variants, splice acceptor and donor site variants, and insertion/deletion polymorphisms. The identified variants were filtered by a frequency of less than 1% in the 1000 Genomes project (http://www.1000genomes.org) and the Human Genetic Variation Browser (http://www.genome.med.kyoto-u.ac.jp/SnpDB/about.html). The remained variants were further screened within 212 genes registered as retinal disease-causing genes in the RetNet database updated on March 10, 2014. All remained variants of 30 arRP/spRP patients were summarized in Table S1 in File S1. Selection of disease-causing mutations was restricted to three genetic criteria: first, homozygosity or compound heterozygosity of known arRP-causing mutations; second, compound heterozygosity